Journal of Water Process Engineering 63 (2024) 105545

Contents lists available at ScienceDirect

Journal of Water Process Engineering

journal homepage: www.elsevier.com/locate/jwpe

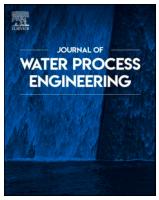

Gravity-driven ultrafiltration and nanofiltration recycled membranes for tertiary treatment of urban wastewater

Bianca Zappulla Sabio, Raquel García Pacheco, Pau Vilardell Pàrraga, Itzel Alcarraz Bernades, Hèctor Monclús Sales, Gaëtan Blandin *

Laboratory of Chemical and Environmental Engineering, Institut de Medi Ambient, Universitat de Girona, Campus Montilivi, C/ Pic de Peguera, 15, La Creueta, 17003 Girona, Spain

ARTICLE INFO

Editor: Tzyy Haur Chong

Keywords:
Gravity-driven membrane
Membrane recycling
Nanofiltration
Ultrafiltration
Water reuse

ABSTRACT

Water scarcity push towards increased number of desalination plants which suppose an exponential increase of end-of-life (EOL) reverse osmosis (RO) membranes. This research is focused on converting EOL RO membranes into ultrafiltration- (UF-like) and nanofiltration-like (NF-like) membranes to be used as tertiary treatment for water reuse. Converted UF- and NF-like membranes were installed in a gravity driven membrane (GDM) setup. The system was fed with secondary effluent of an urban wastewater treatment plant (WWTP) in Girona (Spain), operated during 6 weeks with a driving force of 0,184 bar, applying daily membrane flushing and, chemical cleaning after 2–3 weeks of operation. UF-like membrane achieved permeabilities of 12,2 and 8,8 $L{\cdot}m^{-2}{\cdot}h^{-1}{\cdot}bar^{-1}$ pre- and post-chemical cleaning respectively. NF-like membranes demonstrated also to be of interest for GDM systems, achieving permeabilities of 2,2 and 3,4 $L{\cdot}m^{-2}{\cdot}h^{-1}{\cdot}bar^{-1}$ pre- and post-chemical cleaning respectively. High permeate quality was obtained with turbidity rejection above 87,2 % and *Escherichia coli* (*E. coli*) Logarithmic removal value (LRV) of 4 and 5 for UF-like and NF-like membrane respectively. UF-like and NF-like membranes installed in a GDM system allowed to produce recycled water in accordance with *Real Decreto 1620/2007* positioning it as a low-cost, and compliant solution for water reuse applications.

1. Introduction

Using reverse osmosis (RO) membranes, typically thin-film composite (TFC) membranes with polyamide (PA) as the selective layer is the state-of the art in desalination plants. RO desalination implementation has been widespread around the world due to the increasing need for fresh water. In 2022, 22,757 desalination plants were operating around the world with a total capacity of 212,79 million $m^3{\cdot}day^{-1}$ [1].

Membrane replacement rate is typically of around 20 %, i.e. 5 years lifetime for seawater desalination and could decrease even down to 1–3 years for more challenging stream like landfill leachate [2,3]. This fact, along with the large number of desalination plants that exist nowadays, supposes that more than two millions of RO membranes will be discarded in 2025, which, normally, are incinerated or disposed of in landfills during hundred years until they are degraded [4]. Given the steadily increase of membrane usage and the necessity to move towards a circular economy, there is a crucial need to recycle end-of-life (EOL) discarded membranes. Nowadays options for EOL RO membranes include direct recycling [5,6], regeneration [5], upcycling [5] or to dismantle the components and recycle them independently [7].

The most common methodology consists in recycling membrane modules without being dismantled using strong oxidants to degrade the PA layer. Several studies mentioned for example, the use of potassium permanganate to convert RO membrane into MF-like membranes [2,9] or sodium hypochlorite to convert into nanofiltration-like (NF-like) or ultrafiltration-like (UF-like) membranes depending on the exposure time [8]. Membranes can be also converted using UV irradiation [4,10,11] or gamma irradiation [12–15] but, in this case, membrane modules need to be dismantled. By applying these methods, EOL RO membranes can be reused in various applications like purification of monosaccharides [15], clarification processes [9], water treatment [5,16], landfill leachate treatment [17].

Gravity-driven membrane (GDM) system has been investigated for the past decades [18]. This system allows to filter using solely the gravity-force generated by a water height pressure differential between the feed tank and the permeate outlet without the need of a pressure

* Corresponding author.
E-mail address: gaetan.blandin@udg.edu (G. Blandin).

https://doi.org/10.1016/j.jwpe.2024.105545
Received 1 March 2024; Received in revised form 9 May 2024; Accepted 22 May 2024

pump. Thanks to its easy operation, its lower energy consumption, limited chemicals usage and low but stable flux, GDM systems have gained increased attention in the past years. All these advantages, support the potential of GDM as an alternative to decentralized wastewater (WW) treatment process [18,19]. A summary of past works comparing the type of membrane used, the filtration area, the pressure applied, and the water treated is shown in Table 1. Initially, GDM was implemented to treat drinking water [20], but due to its great functionality, its usage has been extended to other applications like to treat greywater [21–23], surface water [24], groundwater [25], rainwater [26–28], and WW [29–32] or as seawater pretreatment [33]. GDM has been tested even to challenging WW as primary treatment or combined into GDM- membrane bioreactor [34]. GDM system have been also implemented as a household water treatment and safe storage (HWTS) systems for rural areas, isolated areas or in emergency situations. In these cases, the fluxes needed are lower than the ones for industrial applications and most of them uses rainwater as a feed, as shown in the Table 1.

Typically, GDM systems use ultrafiltration (UF) membranes in hollow fiber (HF) [27,28,35] or flat-sheet (FS) [33,36,37] configurations. UF is a perfect candidate for GDM system since it acts as a strong barrier to pathogens and suspended solids and can be operated with low driving force. The installation of these membranes can take two distinct configurations: external [20,29,32] (membrane placed outside the feed water tank) or submerged setup [25,26,33] (membrane placed within the water tank). Each of these configurations presents its own set of advantages and disadvantages. External configuration features easy membrane replacement but pressure vessels, endcaps [17] or fitting system are needed which suppose an extra cost. In external configuration, the membrane is less prone to pollutant deposition but needs larger footprint to install the system (membrane module and tank). Interestingly for EOL membrane, submerged configuration allows to use membrane modules with external damage (due to former usage or factory issue) giving another potential life to membrane that would have been otherwise directly discarded. However, the implementation of the GDM system using 8″ spiral-wound NF-like or UF-like membrane at pilot-scale remains an area yet to be explored.

The aim of this research is to implement an 8″ spiral wound EOL RO membrane converted into UF-like and NF-like membranes in a GDM system as a tertiary WW treatment. UF-like membranes will be assessed in both configurations; external and submerged membranes while NF will be assessed just in external configuration. The experimental setup was located in the wastewater treatment plant (WWTP) of Quart, Girona (Catalonia, Spain) as a tertiary treatment and operated for 6 weeks. This study demonstrated the potential to implement a GDM system using EOL membranes for water reuse on a tertiary effluent and to achieve sustainable operation and permeate quality in line with Spanish law directive.

2. Materials and methodology

2.1. Membranes

4 EOL membranes (CSM NF NE8040 and 3 TORAY RO TML720) and a new but faulty membrane discarded in the manufacturing process (Suez RO AG-400P) were used for this study. The membrane module from Suez RO AG-400P has not been used before. CSM NF-NE8040 and TORAY membranes (RO TML720) were previously used in a pharmaceutical process and to treat secondary urban WW effluent in a golf camp respectively.

All membranes modules received a passive chlorine treatment to be converted into UF-like or NF-like following the procedure from Garcia-Pacheco et al. [50]. A sodium hypochlorite solution was used with a dose

Table 1
Summary of previous works on GDM systems.

Membrane	Membrane state	Pressure (mbar)	Filtration area (m^2)	Operational mode	Feed	Flux ($L{\cdot}m^{-2}{\cdot}h^{-1}$)	Reference
Pristine and EOL RO membrane converted into NF-like and UF-like	Recycled (municipal and industrial)	100–160 and 80	2,23	Vertically submerged and external vertically and horizontally	Synthetic river water	1,92 (100–160 mbar) 1,54 (80 mbar)	[17]
UF flat sheet membranes were UP150 from Microdyn Nadir (150 kDa)	New/virgin	50	0,06	Low-pressure gravity-driven membrane bioreactor (GDMBR) system.	Synthetic grey water	1 (non-aerated) 2 (aerated)	[22]
Hollow fiber high-density polyethylene (pore size of 0,2 μm)	–	300	12	The bioreactor was operated as discontinuously fed process with independent inflow and effluent times	Greywater	1–2	[23]
UF flat sheet membranes were UP150 from Microdyn Nadir (150 kDa)	New	50	0,00125	Decentralized rainwater treatment due to no backwashing, flushing and chemical cleaning	Rainwater	6–6,5 (rainwater) 4 (tap water - control system)	[26]
UF flat sheet polyvinylidene fluoride (250 kDa)	–	40–100	0,00693	Lab-scale submerged GDM systems	Seawater (pretreatment)	7,7 (UF 12 h)| 7,3 (UF 24 h)	[33]
UF flat sheet polymeric membrane (100 kDa)	New (coupon)	50, 70 and 100	0,00221	Back washing and chemical cleaning	Well water contaminated with fecal microorganisms	4,4 (50 mbar) 4,7 (70 mbar) 6,5 (100 mbar)	[36]
UF flat sheet polyethersulfone membrane (100 kDa)	New	65	–	Dead-end without flushing or cleaning	River-, lake- or diluted WW	4–10	[37]
UF flat sheet polyvinylidene fluoride (PVDF) and polyethersulfone (PES) (100 kDa)	New	50 (L) and 150 (H)	–	–	Raw water from the river	4,73 (PVDF-L)| 5,08 (PVDF-H) 3,85 (PES-L)| 4,38 (PES-H)	[40]
UF flat sheet PVC60/PEG400/ZnO 14/10/1	New	78	–	Dead-end mode for 12 h	River water	3	[42]
Hollow fiber Multibore® PES (pore size of 0,02 μm)	New and second-life (5 years)	150	0,22 (new) and 0,20 (second-life)	2 min backwash: No (nBW), every two weeks (2wBW), weekly (wBW) and daily (dBW)| + daily relaxation (R + FF)	River water	1,4 (nBW) 10,6 (dBW) 0,58 (wBW) 0,63 (2wBW)	[45]

of 30.000 ppm·h and 300.000 ppm·h to convert the membranes into NF-like and UF-like respectively. Afterward, the membranes were thoroughly rinsed with DI water. This treatment is based on membrane surface transformation related to the degradation of the polyamide layer, partially and totally to be converted into NF-like and UF-like modules respectively. All the information is summarized in Table 2 including the internal code used during all the experiments. Table 4 shows the performances (permeability and salt rejection) before any treatment applied after its first industrial application. The membranes were characterized under the following conditions: 2000 mg·L^{-1} NaCl feed water, 15 bar, 25 °C and 15 % recovery, in a high-pressure filtration pilot as explained in Section 2.2.1.

2.2. Set-ups

2.2.1. Membrane characterization pilot

Membranes were characterized prior and after the conversion process. Permeability and salt rejection were measured using 2000 mg·L^{-1} NaCl, under 15 bar, 25 °C and 15 % recovery. A schematic diagram of the pilot plant is shown in Fig. 1. It consists in a 1000 L feed tank, a low-pressure pump, high-pressure pump, a pressure vessel to fit one spiral wound 8″ membrane module and an electrical control panel. The feed tank had a conductivity and level sensor recording data during all the process. The salinity was regulated manually by adding salt in the feed tank and checked by a conductivity sensor (4000–5000 μS·cm^{-1}). The pressure was regulated by automatic control of the back-pressure valve located in the retentate pipe and the feed flowrate was controlled using a flowmeter already implemented in the system. Pressure and temperature sensors were installed in the feed line. Permeate and retentate were both sent back to the feed tank to operate at constant feed salinity. Both permeability and rejection coefficients were calculated after at least 30 min of filtration.

2.2.2. Gravity driven membrane pilot tests

The GDM setup was located at Quart WWTP, Girona (Spain) which has a biological treatment and low-loaded activated sludge to treat municipal WW from Quart and surroundings with a capacity of 600 m^3·day^{-1}. The system was fed with the secondary effluent, i.e., supernatant from the clarifier. Two different filtrations set up allowed to test recycled membranes: in an external configuration and a submerged one. CSM NFe, SUEZ UFe, TORAY NFe and TORAY UFe membranes were tested in external configuration and the TORAY UFi as internal configuration.

For the external configuration, the membrane was installed with polyvinyl chloride (PVC) end-caps [17] in a vertical configuration next to the feed tank. The end-caps design includes a mechanical fixing to fit with the membrane module and avoid leakage between the feed and the permeate. For the internal/submerged configuration, only a simple fitting needs to be installed and connected to the membrane module

Table 2
Membranes used in the experiments.

Manuf.	Original model	Internal code	Area (m^2)	Treated water	First industrial application
Suez	RO AG-400P	Suez UFe	37	None	Never industrially used Operating life-span: 0 years
CSM	NF NE8040	CSM NFe		Well water	Pharmaceutical process Operating life-span: 3 years
Toray	RO TML720	Toray UFi Toray UFe Toray NF		Secondary urban WW effluent	Reclaiming water for a golf camp irrigation Operating life-span: 5–10 years

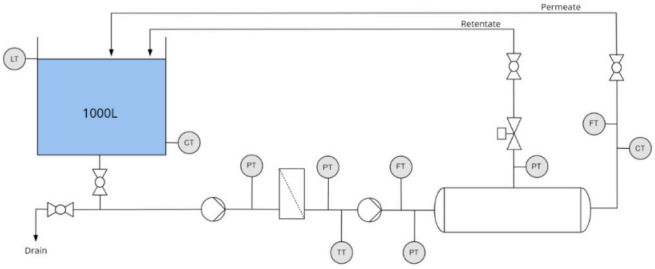

Fig. 1. Schematic diagram of the high-pressure filtering system (FT – flow sensor, PT – pressure sensor, CT – conductivity sensor, LT – level sensor and TT – temperature sensor).

permeate tube (a plug and an outlet fitting to collect the water). In this case, the feed water filled the tank and all the membrane modules while the treated water was collected using the permeate tube.

Fig. 2 shows the distribution of the setup for the experiments with three membranes. The feed tank had one outlet in the top, one inlet in the middle and two outlets in the bottom. The outlet at the top served as overflow to maintain constant water level i.e., constant pressure. Feedwater, i.e., secondary effluent of the WWTP, was injected from the middle inlet. The two outlets at the bottom, fed the two membranes in external configuration.

The GDM set up operation consisted in three successive steps: (1) filtration during 24 or 72 h (during weekends) with the permeate valve opened and a transmembrane pressure (TMP) of 0,184 bar, (2) 10 min of relaxation by closing permeate valves and (3) flushing sequence of 5 min. The flushing was different for external or internal configuration. In the case of the external configuration, the flushing consisted in connecting the effluent from the WWTP directly to the bottom of the membrane module with the flushing valve opened and the permeate one closed. The flushing was implemented in the same direction as the flow in filtration mode, from the bottom to the top, in order to remove the biofilm generated inside the membrane. For the internal configuration, flushing consisted in emptying the feed tank and refilling it with the secondary treated WW.

The experiment was divided into 2 phases, each one lasting about 2–3 weeks as shown on Table 3. The first one was performed directly after membrane module conversion process and the second one after chemical cleaning of the membrane module after 2–3 weeks of operation in the GDM pilot. Chemical cleaning consisted in circulating a free chlorine solution of 500 ppm through the membrane modules during 1,5 h (total dose of 750 ppm·h) [38]. This total exposure dose to free chlorine was selected to do not overtake the limit of exposure for polyamide membrane according to the manufactures (1000 ppm·h) [39].

2.3. Evaluation of membrane performance

2.3.1. Permeate flux and permeability

The permeate flux (J) in GDM tests was assessed while operating with WW by volumetrically measuring the permeated volume (using a 2 L container and stopwatch) and using Eq. (1). This process was repeated five times to determine the standard deviation and was done each day before and after flushing sequence. In Eq. (1), J is the permeate flow (L·h^{-1}), V is the permeated volume (L) and t is the time needed to fill 2 L (h).

$$J = V \Big/ t\left[\frac{L}{h}\right] \tag{1}$$

Permeability (J') was determined using Eq. (2) based on permeate flux, membrane characteristics and pressure in GDM system.

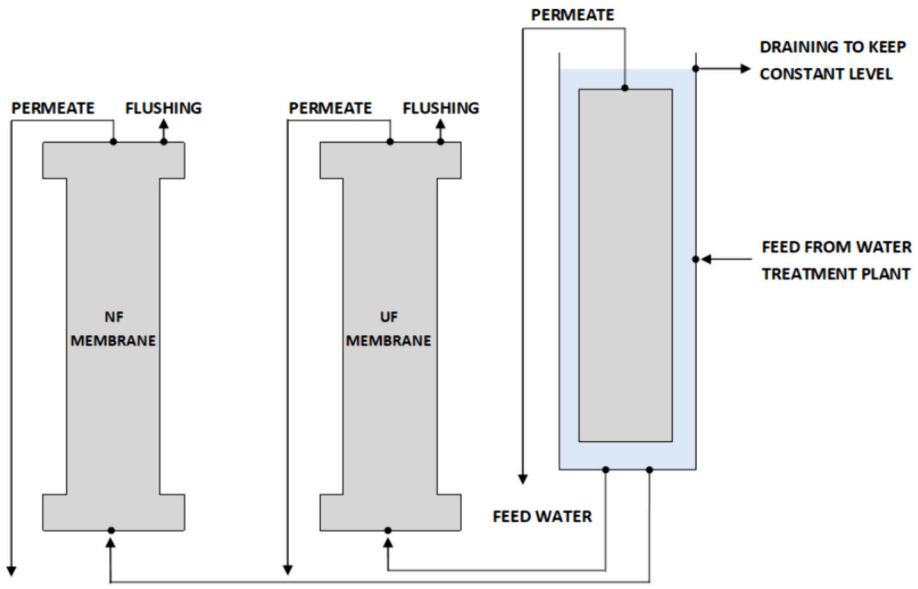

Fig. 2. Schematic diagram of the experimental setup installed to test 3 membranes, two in external configuration one in submerged mode.

Table 3
Summary of operation time and modules used during the GDM pilot tests.

Cycle	After conversion (1)		After chemical cleaning (2)	
Experimental time (days)	12	23	20	19
Membranes used	SUEZ UFe CSM NFe	TORAY UFi TORAY UFe TORAY NFe	SUEZ UFe	TORAY UFi TORAY UFe TORAY NFe

$$J' = J \Big/ (A \cdot \Delta P) \left[\frac{L}{m^2 \cdot h \cdot bar}\right] \tag{2}$$

where J' is the permeability ($L \cdot m^{-2} \cdot h^{-1} \cdot bar^{-1}$), A is the effective membrane filtration area (m^2) and ΔP is the transmembrane pressure (bar). A temperature correction factor (TCF) was applied to normalize the value of permeability at 25 °C. The TCF was calculated as the average of three different equations as shown in Eq. (3) where TCF is the temperature correction factor and T is the temperature of the water from the permeate (°C).

$$\overline{TCF} = \frac{1,002 \cdot e^{3,056 \cdot \left(\frac{25-T}{T+105}\right)} + 1,03^{(25-T)} + \frac{1}{e^{3020 \cdot \left(\frac{1}{298} - \frac{1}{273+T}\right)}}}{3} [-] \tag{3}$$

Finally, the corrected permeability was calculated using Eq. (4) where J'_{corr} is the corrected permeability ($L \cdot m^{-2} \cdot h^{-1} \cdot bar^{-1}$).

$$J'_{corr} = J' \cdot \overline{TCF} \left[\frac{L}{m^2 \cdot h \cdot bar}\right] \tag{4}$$

For GDM, the TMP was calculated directly by the height difference of the system as shown in Eq. (5). H is the height difference between the feed tank and the permeate outlet from the system (m) and 10,2 represents the conversion factor between meter column of water (m.c.a) and bars.

$$\Delta P_{long-term} = H/10,2 [bar] \tag{5}$$

For membrane characterization in high pressure setup, same equations as for GDM were used and TMP was determined through Eq. (6). P_{feed}, $P_{retentate}$ and $P_{permeate}$ being the pressure in the feed, retentate and permeate lines respectively.

$$\Delta P_{short-term} = \left(P_{feed} + P_{retentate}\right)/2 - P_{permeate} [bar] \tag{6}$$

2.3.2. Rejection coefficients

Rejection was calculated using Eq. (7) with C_o the feed concentration and C_p the concentration in the permeate. Rejection coefficients were calculated for salts (conductivity) and turbidity.

$$\%R = 1 - C_o/C_p [\%] \tag{7}$$

2.4. Water quality analysis

Physical-chemical and microbiological quality of feed and permeates from each membrane module in GDM operation were analyze two times per week.

2.4.1. Physical-chemical parameters

Conductivity and pH were measured using Hach SensION+ EC7 and PH3 equipment, respectively. Turbidity was measured using a Portable Turbidity Meter from Hanna. Chemical Oxygen Demand (COD) was measured using the Lovibond DQO MD 110 equipment and HR 200–15,000 $mg \cdot L^{-1}$ kits. Total Organic Carbon (TOC) was measured using the Hach spectrophotometer DR3900 and the LCK387 kits. Cations and anions were measured using Dionex Ion Chromatography equipment.

2.4.2. Microbiological parameters

100 mL of permeate was filtered using a Büchner funnel with a cellulose nitrate filter with 0,45 μm pores. The filter was then placed into Chromogenic Coliform Agar (CCA) plates, which serve as a selective medium for coliform bacteria. This media allows to differentiate between colonies of *Escherichia coli* (*E. coli* - identified by their blue color) and other coliforms (identified by their pink color). Afterward, the plates were incubated at 37 °C for 24 h. Following incubation, the quantification of blue and pink colonies was performed. The total count of colonies allowed to determine the concentration of total coliform bacteria in the sample, expressed as Colony-Forming Units (CFU) per 100 mL. For feed samples, a 1:100 dilution was done and inoculated directly onto the plate without filtering. Logarithmic removal value (LRV) was performed to calculate the membrane rejection in base 10 by comparing feed and permeate water. To determine the *E. coli*, other coliforms and total coliforms LRV, Eq. (8) was used.

$$LRV = log\left(CFU_{permeate}/CFU_{feed}\right)[-] \quad (8)$$

Finally, with Eq. (9), the percentage of rejection of coliforms was calculated.

$$\%Rejection = \left(CFU_{feed} - CFU_{permeate}\right)/CFU_{feed}\cdot 100[\%] \quad (9)$$

3. Results and discussion

3.1. Membrane characterization

Permeability and salt rejection before and after the conversion process are shown in Table 4. As seen on Table 4, the membrane with higher permeability after conversion is the SUEZ UFe. This difference on permeability can be related to the fact that this membrane has never been used before and, consequently, has not been compacted unlike the ones used in industry for years [51]. After conversion, membranes were in the same range as observed with similar treatment in the literature. In the case of the SUEZ UFe membrane, Moreira et al. [46] found a comparable increase in permeability, achieving a permeability of 50,4 $L{\cdot}m^{-2}{\cdot}h^{-1}{\cdot}bar^{-1}$ after converting an EOL membrane with initially permeability of 4,5 $L{\cdot}m^{-2}{\cdot}h^{-1}{\cdot}bar^{-1}$into UF. Regarding the membranes from TORAY, converted into UF-like membranes (UFe and UFi), the values of permeability achieved after conversion were 11,5 and 26,7 $L{\cdot}m^{-2}{\cdot}h^{-1}{\cdot}bar^{-1}$ respectively. Notably, despite originating from the same production facility and sharing identical model specifications, there exists considerable disparity in the achieved permeability values. This discrepancy becomes more pronounced when comparing with the results obtained by Molina et al. [47] using the same TORAY TM720-400 membrane. Molina et al. [47] achieved a significantly higher permeability of 274,6 $L{\cdot}m^{-2}{\cdot}h^{-1}{\cdot}bar^{-1}$. It is crucial to note that Molina et al. [47] experiments were conducted under different conditions, i.e. utilizing a membrane coupon, operating at 5 bar pressure, and employing distilled water for permeability determination. These variations in experimental parameters likely contribute to the observed differences in permeability values. Furthermore, the permeability values obtained in this study for recycled NF membranes are comparatively lower than those reported by García-Pacheco et al. [49] using the TORAY TM720–400 membrane. In their study, [49] a permeability of 14 $L{\cdot}m^{-2}{\cdot}h^{-1}{\cdot}bar^{-1}$ was achieved after exposure to a free chlorine dose of 6200 ppm·h. However, in another study by García-Pacheco et al. [50] employing the same membrane, permeability values of 7,4 $L{\cdot}m^{-2}{\cdot}h^{-1}{\cdot}bar^{-1}$ after 20 h of exposure to a 124 ppm free chlorine solution, and 17,2 $L{\cdot}m^{-2}{\cdot}h^{-1}{\cdot}bar^{-1}$ after 50 h were obtained. Once again, it is important to consider that García-Pacheco et al. [50] conducted their experiments using coupon specimens, which may exhibit distinct behavior compared to the entire module, potentially influencing membrane permeability.

3.2. Gravity driven membrane filtration tests

As shown in Table 3, the experiment was divided into 2 cycles: (1) after the conversion process and (2) after the chemical cleaning. The membranes used in each cycle were the same and in the same configuration (vertically submerged or external) so to comparatively assess the impact of chemical cleaning.

3.2.1. Permeability

This investigation demonstrated the feasibility of WW filtration employing recycled modules within a GDM system, operating under a TMP of 0,184 bar. Fig. 3 shows the permeability of the membranes across both experimental cycles, pre- (light color circles) and post- (dark color squares) daily flushing procedures. Blue dots represent data points obtained after the conversion process cycle, while green dots indicate observations following chemical cleaning. The delineated grey markers denote the specific day of chemical cleaning execution. The SUEZ UFe and CSM NFe membranes were subjected to testing in a vertically external configuration for a duration of 12 days following the conversion process, and afterward, for an additional 20 days post-chemical cleaning. Unfortunately, the CSM NFe broke during the transport and could not be installed in the second cycle. Conversely, membranes sourced from TORAY, including both UFe and NFe variants, underwent assessment in an external configuration, while the UFi variant was evaluated in a submerged configuration. All TORAY membranes were subjected to testing for 23 days after the conversion process and an additional 19 days following chemical cleaning.

During the initial phase of experimentation, the Suez UFe membrane exhibited a stable permeability levels pre-flushing, followed by a subsequent increase after flushing. However, post-application of chemical cleaning, this trend reversed, with permeability showing a decline in both pre- and post-flushing states. In contrast, TORAY membranes maintained a constant behavior throughout the experimental duration. This discrepancy may be attributed to the prior history of the membranes, where the SUEZ UFe had not been previously employed while the TORAY UFe had been used and can be compacted. The average permeability for the SUEZ UFe was around 12,2 $L{\cdot}m^{-2}{\cdot}h^{-1}{\cdot}bar^{-1}$ (2,2 $L{\cdot}m^{-2}{\cdot}h^{-1}$) after the conversion process and around 8,7 $L{\cdot}m^{-2}{\cdot}h^{-1}{\cdot}bar^{-1}$ (1,6 $L{\cdot}m^{-2}{\cdot}h^{-1}$) after the chemical cleaning. These values exceeded those obtained for TORAY membranes in this experiment, because of the pristine condition of the SUEZ membrane. For the TORAY UFe membrane, the permeability post-conversion was approximately 10,2 $L{\cdot}m^{-2}{\cdot}h^{-1}{\cdot}bar^{-1}$ (1,9 $L{\cdot}m^{-2}{\cdot}h^{-1}$), diminishing to around 8,5 $L{\cdot}m^{-2}{\cdot}h^{-1}{\cdot}bar^{-1}$ (1,6 $L{\cdot}m^{-2}{\cdot}h^{-1}$) after chemical cleaning. Conversely, for the submerged membrane (TORAY UFi) the values were 3,8 $L{\cdot}m^{-2}{\cdot}h^{-1}{\cdot}bar^{-1}$ (0,7 $L{\cdot}m^{-2}{\cdot}h^{-1}$) and 3,4 $L{\cdot}m^{-2}{\cdot}h^{-1}{\cdot}bar^{-1}$ (0,6 $L{\cdot}m^{-2}{\cdot}h^{-1}$) respectively. The values achieved by the TORAY UFi are lower for an UF membrane but demonstrate that even if the membrane has external damage, it can be used in a GDM system. As reported by Garcia-Pacheco et al. [17] submerged membranes demonstrated inferior permeability compared to externally positioned membranes, likely due to higher sensibility to contaminants from the WWTP residing in the feed tank, leading to fouling and subsequent permeability reduction. Comparing results with NF membranes, the CSM NFe membrane exhibited an average permeability of approximately 2,9 $L{\cdot}m^{-2}{\cdot}h^{-1}{\cdot}bar^{-1}$ (0,5 $L{\cdot}m^{-2}{\cdot}h^{-1}$) post-conversion, whereas the TORAY NFe membrane recorded approximately 2,3 $L{\cdot}m^{-2}{\cdot}h^{-1}{\cdot}bar^{-1}$ (0,4 $L{\cdot}m^{-2}{\cdot}h^{-1}$). Post-chemical cleaning, the TORAY NFe membrane demonstrated an unexpected increase in permeability to approximately 3,4 $L{\cdot}m^{-2}{\cdot}h^{-1}{\cdot}bar^{-1}$ (0,6 $L{\cdot}m^{-2}\cdot h^{-1}$), surpassing conventional NF membrane expectations and suggesting partial conversion into UF performance. This observation and the trend of membrane permeability decline post-chemical cleaning for all the membranes except for the TORAY NFe, confirmed the partially conversion of this membrane into UF-like membrane.

Table 1 presents an overview of flux values attained in GDM systems

Table 4
Permeability and salt rejection before and after the conversion process.

	Membrane	Suez UFe	Toray UFe	Toray UFi	CSM NFe	Toray NFe
EOL membrane performance (before conversion)	Permeability ($L{\cdot}m^{-2}{\cdot}h^{-1}{\cdot}bar^{-1}$)	2,15	1,9	1,6	4,5	2,5
	Salt rejection (%)	99,8	96,7	93,6	99,1	97,6
After conversion	Permeability ($L{\cdot}m^{-2}{\cdot}h^{-1}{\cdot}bar^{-1}$)	50,7	11,5	26,7	6,1	3,2
	Salt rejection (%)	24,6	31,4	24,8	96,0	96,3

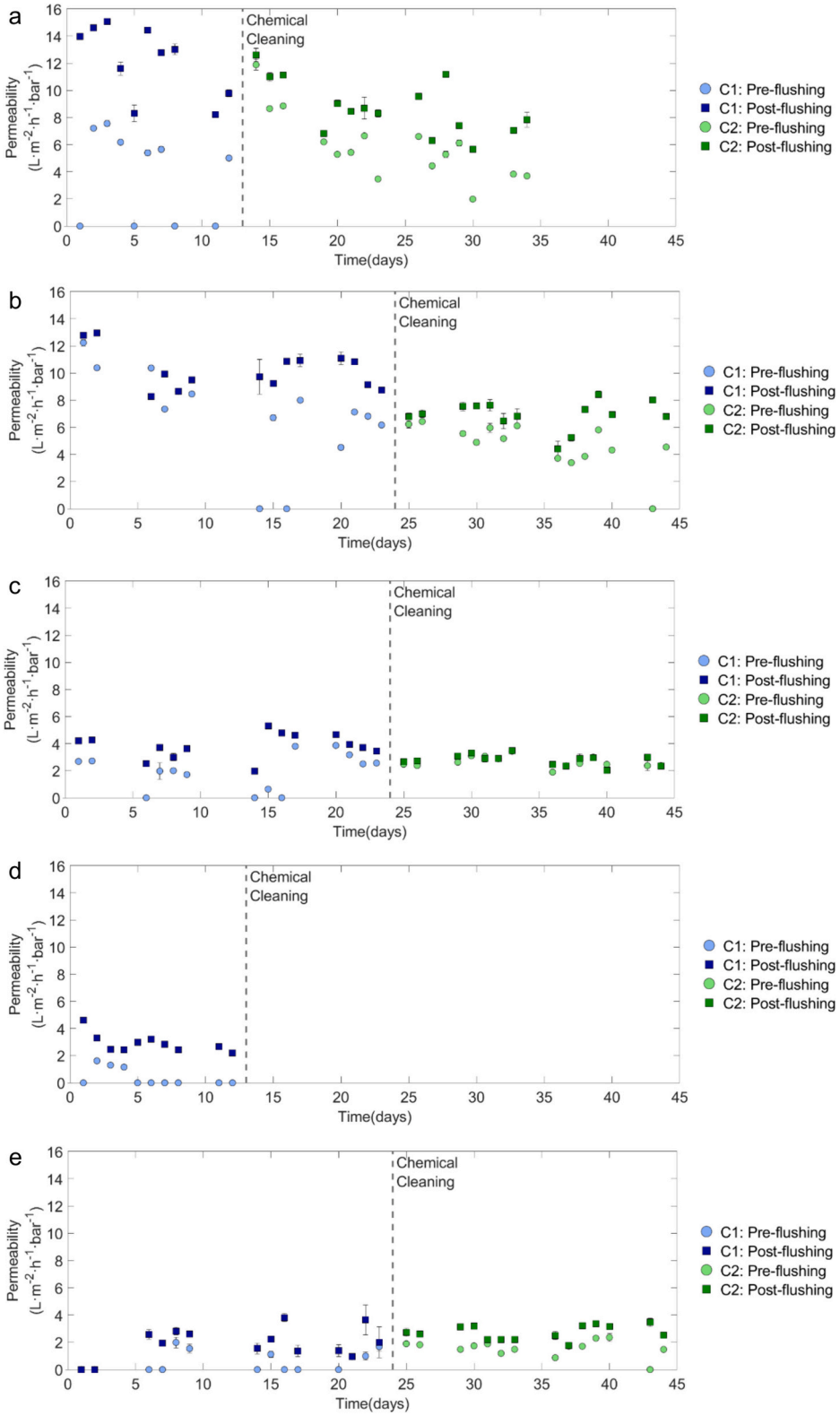

Fig. 3. Permeability dynamics of the membranes (a. Suez UFe, b. Toray UFe, c. Toray UFi, d. CSM NFe, e. Toray NFe) across both experimental cycles, pre- (light color circles) and post- (dark color squares) daily flushing procedures. Blue dots: after the conversion process, green dots: after the chemical cleaning process, dash line: chemical cleaning day. The CSM NFe broke during the transport and could not be installed in the second cycle.

utilizing both new UF flat sheet membranes and converted EOL RO membranes. Disparities in flux among different membranes can be attributed to membrane composition and configuration. In cases of higher water contamination, flux tends to diminish due to fouling accumulation on the membrane surface. Additionally, the applied pressure directly influences the achievable flux rate of the membrane. The flux values obtained with UFe membranes (SUEZ and TORAY) exhibit similarity to those reported by Wang et al. [30], García-Pacheco

et al. [17] and Ding et al. [22] but are lower compared to Peter-Varbanets et al. [37], de Souza et al. [36], Teta Prihartini et al. [42] and Ranieri et al. [33]. These discrepancies primarily are resulting from the utilization of used membranes in contrast to pristine, uncompacted new ones. Conversely, the installation of NF membranes in GDM systems represents a relatively novel or less-studied approach and, the utilization of recycled NF-like membranes represents a particularly innovative application. Although the implementation of these recycled NF-like membranes appears promising, filtration over extended periods necessitates daily flushing to mitigate fouling. Comparing with the values achieved by Garcia-Pacheco et al. [17], the permeability attained in their study exceeded that of the present experiment. Employing a TORAY TM720-400 membrane converted into NF-like, they achieved a remarkably high permeability value of 14 $L \cdot m^{-2} \cdot h^{-1} \cdot bar^{-1}$, elevated for an NF membrane.

3.2.2. Water quality

The assessment of water quality of the permeates (tertiary effluent) and the feed water (secondary effluent) was conducted in order to evaluate if permeate quality was in accordance with the regulatory limits stipulated in the *Real Decreto 1620/2007* [53]. This directive set out maximum acceptable value (MAV) for various parameters including *E. coli*, suspended solids (SS) and turbidity levels in the context of water reuse. For urban uses like landscape irrigation, the MAV are 200 $CFU \cdot 100\ mL^{-1}$ for *E. coli*, 20 $mg \cdot L^{-1}$ for SS and 10 NTU for turbidity. Additionally, pH and conductivity analyses were performed, revealing negligible changes between the feed and permeate samples. The UF membrane filtration exhibits minimal variations in pH and conductivity, both below 1 %. Specifically, pH remains stable at approximately 7,3, while conductivity stays close around 1300 $\mu S \cdot cm^{-1}$. Conversely, the NF membranes show slightly higher fluctuations, with pH changing by approximately 2 % to 7,2 and conductivity decreasing by 3 % to approximately 1200 $\mu S \cdot cm^{-1}$in the permeate. This outcome was anticipated for the UF-like membrane because it exhibits minimal ion rejection capability, thus exerting minimal influence on these parameters. In the case of NF-type membranes, the conductivity values may remain comparable between the feed and permeate due to the development of a boundary layer near the membrane surface known as concentration polarization (CP) [17,52]. This phenomenon involves the accumulation of retained solutes in the membrane, leading to a higher solute concentration at the membrane surface compared to the bulk solution. Consequently, rejection values and flux may decrease due to the rise in osmotic pressure.

Table 5 presents turbidity values (expressed in nephelometric turbidity units, NTU) for both the feed and permeate samples, alongside the corresponding turbidity rejection percentages for each recycled membrane across both pre- and post-chemical cleaning cycles.

Regarding turbidity values, all the permeates complied with the *Real Decreto 1620/2007* [53] directive for water reuse with values below 10 NTU. The CSM NFe membrane, due to its higher selectivity, shows a superior membrane rejection capacity. Conversely, the TORAY UFi membrane, likely owing to its submerged configuration and consequent heightened exposure to contaminants, exhibited a lower membrane rejection rate. The CSM NFe membrane was the most effective in term of contaminants rejection, but its flux collapsed easily showing limitation in continuous filtration without cleaning during all day. Following closely in terms of contaminants rejection efficiency, the TORAY UFe membrane demonstrates good filtering capacity and continuous filtration throughout each operational day.

To facilitate microbiological analysis, samples of both, permeate and feed, underwent *E. coli* and coliforms analyses. Subsequently, LRV were computed to assess the efficacy of contaminant removal by the membranes. It is essential to note that external factors such as temperature can impact the composition of the feed, especially since it consists of real secondary effluent from the WWTP. On average the feed for the membrane system, exhibited total coliform counts of approximately $1{,}8 \cdot 10^6$ $CFU \cdot 100\ mL^{-1}$ for the experiments prior chemical cleaning and $4{,}2 \cdot 10^4$ $CFU \cdot 100\ mL^{-1}$ after the chemical cleaning. Such a substantial difference could significantly impact the LRV values obtained. The LRV results for *E. coli* and coliforms are presented in Fig. 4.

Analyzing the results pertaining to other coliforms, it was observed that all membranes, with the exception of the SUEZ UFe prior to chemical cleaning, exhibited values exceeding 200 $CFU \cdot 100\ mL^{-1}$. Despite this, these values remained lower than those observed in the feed water, indicating a partial rejection of coliforms by the membranes. For *E. coli*, the rejection proved to be notably more effective, with values falling below 20 $CFU \cdot 100\ mL^{-1}$, i.e., limit for the water reuse for irrigation. Especially, the UF TORAY internal and external membrane permeates exhibited *E. coli* results surpassing 200 $CFU \cdot 100\ mL^{-1}$. Comparing with findings from the study conducted by Figueras et al. [44], the *E. coli* rejection rates for SUEZ UFe, CSM NFe, and TORAY UFi membranes were slightly lower but still within the bounds defined by regulatory standards (*Real Decreto 1620/2007* [53]). In the case of the TORAY UFe, the rejection before the chemical cleaning was lower in this experiment but after the chemical cleaning, was higher than the one achieved by Figueras et al. [44]. Remarkably, the TORAY NFe membrane exhibited the highest *E. coli* removal capacity, achieving complete removal pre-chemical cleaning and near-total removal post-cleaning. These results aligned closely with those obtained by Figueras et al. [44] using the TW30 module (RO recycled module). NF-type membranes appear to be a favorable option for achieving higher LRV values compared to UF-type membranes. Despite bacterial presence observed in the permeate, this technology manages to significantly improve water quality (Log LRV of 4–5). Exploring its efficiency across diverse water sources could unveil its potential for household applications such as cleaning, hygiene, and drinking.

Comparing the Spanish law (*Real Decreto 1620/2007* [53]) with the Regulation (EU) 2020/741 [54] of the European parliament and of the council of 25 May 2020 on minimum requirements for water reuse, different MAV have been observed. For irrigation water where the edible part is in direct contact with reclaimed water, the EU 2020/741 [54] is stricter than the *Real Decreto 1620/2007* [53]. When comparing turbidity values, the EU 2020/741 [54] for water reuse imposes a stricter limit of 5 NTU compared to the *Real Decreto 1620/2007* [53], which allows up to 10 NTU. All samples met both criteria. Regarding *E. coli* levels, the EU 2020/741 [54] for water reuse mandates a lower threshold of 10 CFU/100 mL, whereas the *Real Decreto 1620/2007* [53] permits up to 100 CFU/100 mL. In the initial cycle, SUEZ and TORAY NFe membranes met the requirement, with *E. coli* levels below 10 CFU/100 mL, while TORAY UF membranes exceeded this threshold. In the subsequent cycle, all TORAY membranes fit with the EU 2020/741 [54] limit, while the SUEZ membrane recorded a value exceeding it. Overall,

Table 5
Turbidity of the feed and permeates and, the turbidity rejection of the recycled membranes tested for both cycles, prior and after applying the chemical cleaning.

		Feed	Permeate				
	Membrane	–	Suez UFe	Toray UFe	Toray UFi	CSM NFe	Toray NFe
Prior chemical cleaning	Turbidity (NTU)	8,1 ± 4,9	1,0 ± 0,8	0,6 ± 0,3	1,8 ± 1,0	0,3 ± 0,1	0,7 ± 0,5
	Turbidity rejection (%)	–	87,2	94,6	82,8	96,6	93,9
After chemical cleaning	Turbidity (NTU)	10,3 ± 8,4	0,6 ± 0,3	4,2 ± 2,5	3,5 ± 2,1	–	4,1 ± 2,1
	Turbidity rejection (%)	–	94,5	56,0	63,3	–	57,0

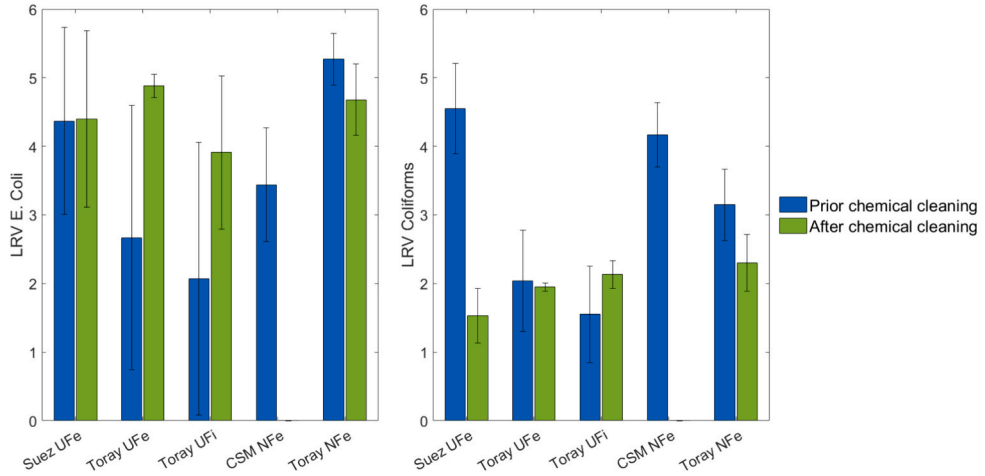

Fig. 4. LRV results for microbiological analysis for both cycles. *Escherichia coli* (left) and other coliforms (right).

permeate quality fit with the requirements of the *Real Decreto 1620/2007* [53] but in some cases did not comply with the more stringent EU 2020/741 [54] with regards to *E. coli* showing the necessity to perform further tests for broader acceptance of the technology.

3.2.3. Cleaning impact

Internal chemical cleaning [38] and external cleaning utilizing pressurized water were conducted to mitigate the biofilm accumulation observed after 12 days of operation within the GDM system. Also, the permeate tubes underwent chemical cleaning to disinfect them, preparing for the second phase of the experiment under conditions akin to cycle 1. Fig. 5 visually depicts the condition of the membranes before (a and c) and after (b and d) external cleaning, focusing on the SUEZ UFe (a and b) and CSM NFe (c and d) membranes. The GDM filtration configuration promotes the development of a biofilm layer within the membranes, forming a "mini ecological system" that contributes to stable flow rates [24]. This phenomenon arises from the accumulation of microorganisms, organic aggregates, colloidal material, and particulate organic and inorganic substances on the membrane surface. Such biofilm accumulation is evident in Fig. 5a and c.

The anticipated accumulation of foulants on the membranes was displayed by a decrease in permeability across all tested membranes. Employing a daily flushing procedure, incorporating both relaxation and flushing cycles, is expected to reduce the fouling tendency of the membrane and allowed to recover partially the initial permeability to avoid the total clogging of the membrane. After the chemical cleaning, the permeability did not come back to the initial state but showed less difference before and after the flushing which suppose a more stable values of permeability.

Considering values of turbidity, in the case of TORAY membranes, chemical cleaning had a harmful effect on membrane rejection capabilities, resulting in diminished capacity to reject contaminants. Conversely, the SUEZ UFe membrane exhibited a completely opposite result achieving a rejection rate of 94,5 %, akin to that of the TORAY UFe membrane before chemical cleaning. These findings highlight how easily membranes can be damaged by chemical cleaning. Various factors, including drying, foulants, and chemical exposure during membrane usage, contribute to membrane degradation, rendering them more susceptible to treatments such as chemical cleaning. However, the underlying mechanisms governing these phenomena and the resulting alterations in membrane performance remain areas yet to be thoroughly explored.

On the contrary, concerning the LRV values, there has been an uptick in *E. coli* rejection observed with the TORAY membranes following chemical cleaning, while coliform rejection shows less impact. This observation can be linked to the chemical cleaning of the tubes. At the end of Cycle 1, due to usage and climatic conditions, the values of *E. coli* obtained were higher than the initial ones. This trend is affirmed by the increased *E. coli* rejection on the permeate sample, due to the decrease in *E. coli*, seen in Cycle 2.

In conclusion, while chemical cleaning had a discernible impact on membrane performance, it proved to be insufficient for complete restoration of initial performance levels. Moreover, the tube cleaning has proven to be effective in microbiological rejection.

4. Conclusion

This study demonstrated the potential of integrating UF-like and NF-like membranes, repurposed from EOL RO membranes, within GDM systems to obtain reused water that fil existing directive (*Real Decreto 1620/2007* [53]) for water reuse.

Among the membranes evaluated in the GDM system, the SUEZ UFe emerged as the most efficient, achieving an average permeability of 10 $L{\cdot}m^{-2}{\cdot}h^{-1}{\cdot}bar^{-1}$ across both cycles and continuous filtration for up to 72 h. Moreover, this membrane exhibited high turbidity removal (90 %) and substantial reduction in *E. coli* and coliforms. The TORAY UFe presented the most promising overall performance with consistent filtration throughout all day and turbidity rejection rate of 94,6 % (pre-chemical cleaning) and 56 % (post-chemical cleaning), alongside *E. coli* LRV of 2,7 (increasing to 4,9 post-chemical cleaning) and coliforms LRV of 2 before and after chemical cleaning. Once more, the rise in LRV value after chemical cleaning can also be attributed to the reduction in

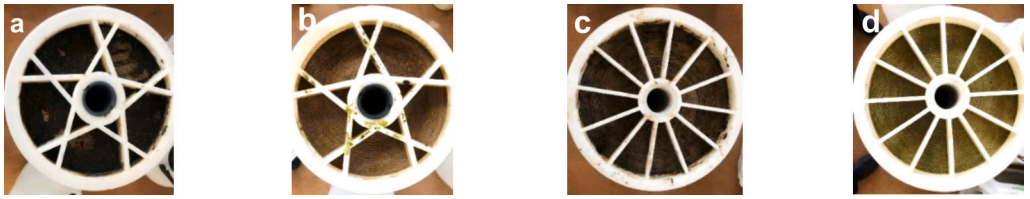

Fig. 5. Membranes before and after the cleaning process: a) SUEZ UFe before, b) SUEZ UFe after, c) CSM NFe before and d) CSM NFe after.

coliform composition within the feed.

Furthermore, our findings highlight the potential of NF-like membranes in GDM systems with the limitation of needing daily flushing to maintain filtration capability.

The results obtained also suggest that the permeate water quality from both, converted new but faulty discarded from manufacturer and EOL membranes, is suitable for water reuse. Despite bacterial presence (LRV of 4–5) observed in the permeate, this finding underscores the effectiveness of these membranes in treating WWTP effluent and significantly enhancing water quality. These findings warrant further exploration in other water sources to see their efficiency and to validate the efficacy of this system for household water treatment and for obtaining drinking water (with a disinfection), especially in remote or emergency settings.

In conclusion, the integration of discarded and recycled 8″ EOL RO membranes, repurposed into UF-like or NF-like membranes, into GDM systems showcases the potential of this approach for effective tertiary WW treatment. Future research will focus on long-term experiments incorporating automated control systems for permeate flux, alongside optimization of flushing/cleaning procedures to define an optimal protocol and to assess the impact of multiple chemical cleaning on process performances.

Funding and acknowledgments

We would like to thank the wastewater treatment plant of Quart to let us do all the experimental part there. This work was funded by MCIN/AEI/10.13039/501100011033 (OSMO4LIVES). We gratefully acknowledge the financial support. Bianca Zappulla received the support of a FI-SDUR predoctoral aid program of the Department of Research and Universities of the *Generalitat de Catalunya* (AGAUR) [REF: 2023 FISDU 00267]. Gaetan Blandin received the support of a fellowship from "la Caixa" Foundation (ID 100010434) [REF: LCF/BQ/PR21/11840009]. Raquel García Pacheco acknowledges to MEM4ALL project granted by Plan Estatal de Investigación Científica y Técnica y de Innovación 2017–2020, Ayudas Juan de la Cierva—Incorporación-2020 IJC2020-044238-I/MCIN/AEI/10.13039/501100011033 and European Union "NextGenerationEU/PRTR". Hèctor Monclús acknowledges Agencia Estatal de Investigación of the Spanish Ministry of Science, Innovation and Universities (MCIU) for partially funding this research through the Ramon y Cajal Research Fellowship (RYC2019-026434-I). LEQUiA [2021-SGR-01352] has been recognized as consolidated research group by the Catalan Government.

Open Access funding provided thanks to the CRUE-CSIC agreement with *Elsevier*.

CRediT authorship contribution statement

Bianca Zappulla Sabio: Writing – original draft, Validation, Methodology, Investigation, Formal analysis, Data curation. **Raquel García Pacheco:** Writing – review & editing, Supervision, Conceptualization. **Pau Vilardell Pàrraga:** Methodology. **Itzel Alcarraz Bernades:** Methodology. **Hèctor Monclús Sales:** Writing – review & editing, Supervision. **Gaëtan Blandin:** Writing – review & editing, Supervision, Project administration, Conceptualization.

Declaration of competing interest

The authors declare the following financial interests/personal relationships which may be considered as potential competing interests: Gaetan Blandin is serving as guest editor of the VSI Circularity in separation processes – green, recycled and upcycled materials (membranes, adsorbents, catalysts). However, he was not involved with neither the review process nor the handling of paper. If there are other authors, they declare that they have no known competing financial interests or personal relationships that could have appeared to influence the work reported in this paper.

Data availability

Data will be made available on request.

References

[1] Source: GWI DesalData updated October 2022 and IDA desalination & reuse handbook 2022–2023. https://idadesal.org/.
[2] Y.S. Khoo, W.J. Lau, S.W. Hasan, W.N.W. Salleh, A.F. Ismail, New approach of recycling end-of-life reverse osmosis membranes via sonication for microfiltration process, J. Environ. Chem. Eng. 9 (6) (2021) 106731, https://doi.org/10.1016/j.jece.2021.106731.
[3] W. Lawler, Z. Bradford-Hartke, M.J. Cran, M. Duke, G. Leslie, B.P. Ladewig, P. Le-Clech, Towards new opportunities for reuse, recycling and disposal of used reverse osmosis membranes, Desalination 299 (2012) 103–112, https://doi.org/10.1016/j.desal.2012.05.030.
[4] J. Senán-Salinas, J. Landaburu-Aguirre, J. Contreras-Martinez, E. García-Calvo, Life Cycle Assessment application for emerging membrane recycling technologies: from reverse osmosis into forward osmosis, Resour. Conserv. Recycl. 179 (2022) 106075, https://doi.org/10.1016/j.resconrec.2021.106075.
[5] X. Zheng, Y. Chen, L. Zheng, R. Cheng, H. Hua, Recycling of aged RO membranes as NF/UF membranes: biosafety evaluation and aging process, Desalination 538 (2022) 115845, https://doi.org/10.1016/j.desal.2022.115845.
[6] A. Lejarazu-Larrañaga, J. Landaburu-Aguirre, J. Senán-Salinas, J.M. Ortiz, S. Molina, Thin film composite polyamide reverse osmosis membrane technology towards a circular economy, Membranes 12 (9) (2022) 9, https://doi.org/10.3390/membranes12090864.
[7] S. Guclu, N. Kizildag, B. Dizman, S. Unal, Solvent-based recovery of high purity polysulfone and polyester from end-of-life reverse osmosis membranes, Sustain. Mater. Technol. 31 (2022) e00358, https://doi.org/10.1016/j.susmat.2021.e00358.
[8] C. Tian, Recycling of End-of-Life Polymeric Membranes for Water Treatment: Closing the Loop, 2023.
[9] K. Khaless, B. Achiou, R. Boulif, R. Benhida, Recycling of spent reverse osmosis membranes for second use in the clarification of wet-process phosphoric acid, Minerals 11 (6) (2021) 637, https://doi.org/10.3390/min11060637.
[10] R. García-Pacheco, J. Landaburu-Aguirre, P. Terrero-Rodríguez, E. Campos, F. Molina-Serrano, Rabadán, Validation of recycled membranes for treating brackish water at pilot scale, Desalination 433 (2018) 199–208, https://doi.org/10.1016/j.desal.2017.12.034.
[11] W. Cheng, H. Xu, P. Wang, L. Wang, A. Szymczyk, J.-P. Croué, Modification mechanism of polyamide reverse osmosis membrane by persulfate: roles of hydroxyl and sulfate radicals, Environ. Sci. Technol. 56 (12) (2022) 8864–8874, https://doi.org/10.1021/acs.est.2c00952.
[12] H. Rho, S.-J. Im, O. Alrehaili, S. Lee, A. Jang, F. Perreault, P. Westerhoff, Facile surface modification of polyamide membranes using UV-photooxidation improves permeability and reduces natural organic matter fouling, Environ. Sci. Technol. 55 (10) (2021) 6984–6994, https://doi.org/10.1021/acs.est.0c07844.
[13] C. Liu, J. Zhang, W. Wang, Y. Guo, K. Xiao, Effects of gamma-ray irradiation on separation and mechanical properties of polyamide reverse osmosis membrane, J. Membr. Sci. 611 (2020) 118354, https://doi.org/10.1016/j.memsci.2020.118354.
[14] N. Combernoux, V. Labed, L. Schrive, Y. Wyart, E. Carretier, P. Moulin, Effect of gamma irradiation at intermediate doses on the performance of reverse osmosis membranes, Radiat. Phys. Chem. 124 (2016) 241–245, https://doi.org/10.1016/j.radphyschem.2015.11.017.
[15] N. Combernoux, L. Schrive, V. Labed, Y. Wyart, E. Carretier, P. Moulin, Irradiation effects on RO membranes: comparison of aerobic and anaerobic conditions, Polym. Degrad. Stab. 134 (2016) 126–135, https://doi.org/10.1016/j.polymdegradstab.2016.09.034.
[16] B. Rathnayake, H. Valkama, M. Ohenoja, J. Haverinen, R.L. Keiski, Evaluation of nanofiltration membranes for the purification of monosaccharides: influence of pH, temperature, and sulfates on the solute retention and fouling, Membranes 12 (12) (2022) 12, https://doi.org/10.3390/membranes12121210.
[17] R. García-Pacheco, Q. Li, J. Comas, R.A. Taylor, P. Le-Clech, Novel housing designs for nanofiltration and ultrafiltration gravity-driven recycled membrane-based systems, Sci. Total Environ. 767 (2021) 144181, https://doi.org/10.1016/j.scitotenv.2020.144181.
[18] W. Pronk, A. Ding, E. Morgenroth, N. Derlon, P. Desmond, M. Burkhardt, Gravity-driven membrane filtration for water and wastewater treatment: a review, Water Res. 149 (2019) 553–565, https://doi.org/10.1016/j.watres.2018.11.062.
[19] R. García-Pacheco, A. Galizia, S. Toribio, J. Gabarró, S. Molina, J. Landaburu-Aguirre, Landfill leachate treatment by using second-hand reverse osmosis membranes: long-term case study in a full-scale operating facility, Membranes 12 (11) (2022) 11, https://doi.org/10.3390/membranes12111170.
[20] S. Lee, C. Risold, N. Landolt, S. Hube, M. Burkhardt, B. Wu, Gravity-driven membrane reactor for decentralized wastewater treatment: comparison of reactor configuration and membrane module, J. Water Process Eng. 54 (2023) 104055, https://doi.org/10.1016/j.jwpe.2023.104055.
[21] P.A. Oka, N. Khadem, P.R. Bérubé, Operation of passive membrane systems for drinking water treatment, Water Res. 115 (2017) 287–296, https://doi.org/10.1016/j.watres.2017.02.065.

[22] A. Ding, H. Liang, G. Li, I. Szivak, J. Traber, W. Pronk, A low energy gravity-driven membrane bioreactor system for grey water treatment: permeability and removal performance of organics, J. Membr. Sci. 542 (2017) 408–417, https://doi.org/10.1016/j.memsci.2017.08.037.
[23] S. Jabornig, S.M. Podmirseg, A novel fixed fibre biofilm membrane process for on-site greywater reclamation requiring no fouling control, Biotechnol. Bioeng. 112 (3) (2015) 484–493, https://doi.org/10.1002/bit.25449.
[24] L. Truttmann, Y. Su, S. Lee, M. Burkhardt, S. Brynjólfsson, T.H. Chong, Gravity-driven membrane (GDM) filtration of algae-polluted surface water, J. Water Process Eng. 36 (2020) 101257, https://doi.org/10.1016/j.jwpe.2020.101257.
[25] X. Tang, J. Qiao, J. Wang, K. Huang, Y. Guo, D. Xu, Bio-cake layer based ultrafiltration in treating iron-and manganese-containing groundwater: fast ripening and shock loading, Chemosphere 268 (2021) 128842, https://doi.org/10.1016/j.chemosphere.2020.128842.
[26] A. Ding, J. Wang, D. Lin, X. Tang, X. Cheng, H. Wang, A low pressure gravity-driven membrane filtration (GDM) system for rainwater recycling: flux stabilization and removal performance, Chemosphere 172 (2017) 21–28, https://doi.org/10.1016/j.chemosphere.2016.12.111.
[27] B. Kus, J. Kandasamy, S. Vigneswaran, H.K. Shon, G. Moody, Gravity driven membrane filtration system to improve the water quality in rainwater tanks, Water Supply 13 (2) (2013) 479–485, https://doi.org/10.2166/ws.2013.046.
[28] B. Kus, J. Kandasamy, S. Vigneswaran, H.K. Shon, G. Moody, Household rainwater harvesting system – pilot scale gravity driven membrane-based filtration system, Water Supply 13 (3) (2013) 790–797, https://doi.org/10.2166/ws.2013.067.
[29] M. Peter-Varbanets, K. Dreyer, N. McFadden, H. Ouma, K. Wanyama, C. Etenu, Evaluating novel gravity-driven membrane (GDM) water kiosks in schools. https://repository.lboro.ac.uk/articles/conference_contribution/Evaluating_novel_gravity-driven_membrane_GDM_water_kiosks_in_schools/9589124/1, 2017.
[30] Y. Wang, L. Fortunato, S. Jeong, T. Leiknes, Gravity-driven membrane system for secondary wastewater effluent treatment: filtration performance and fouling characterization, Sep. Purif. Technol. 184 (2017) 26–33, https://doi.org/10.1016/j.seppur.2017.04.027.
[31] I.U.H. Shami, B. Wu, Gravity-driven membrane reactor for decentralized wastewater treatment: effect of reactor configuration and cleaning protocol, Membranes 11 (6) (2021) 6, https://doi.org/10.3390/membranes11060388.
[32] X. Guo, Y. Wang, S. Jiang, Y. Wang, J. Wang, H. Liang, Influence of operation modes on gravity-driven membrane process in treating the secondary effluent: flux improvement and biocake layer property, Chemosphere 310 (2023) 136692, https://doi.org/10.1016/j.chemosphere.2022.136692.
[33] L. Ranieri, R.E. Putri, N. Farhat, J.S. Vrouwenvelder, L. Fortunato, Gravity-Driven Membrane as seawater desalination pretreatment: understanding the role of membrane biofilm on water production and AOC removal, Desalination 549 (2023) 116353, https://doi.org/10.1016/j.desal.2022.116353.
[34] L. Fortunato, L. Ranieri, V. Naddeo, T. Leiknes, Fouling control in a gravity-driven membrane (GDM) bioreactor treating primary wastewater by using relaxation and/or air scouring, J. Membr. Sci. 610 (2020) 118261, https://doi.org/10.1016/j.memsci.2020.118261.
[35] D. Stoffel, E. Rigo, N. Derlon, C. Staaks, M. Heijnen, E. Morgenroth, Low maintenance gravity-driven membrane filtration using hollow fibers: effect of reducing space for biofilm growth and control strategies on permeate flux, Sci. Total Environ. 811 (2022) 152307, https://doi.org/10.1016/j.scitotenv.2021.152307.
[36] F.B. de Souza, R.A. Teixeira, S.W. da Silva, A.D. Benetti, Influence of pressure in a point-of-use treatment of well water using gravity-driven ultrafiltration membranes for drinking purposes in developing countries, J. Water Process Eng. 53 (2023) 103645, https://doi.org/10.1016/j.jwpe.2023.103645.
[37] M. Peter-Varbanets, F. Hammes, M. Vital, W. Pronk, Stabilization of flux during dead-end ultra-low-pressure ultrafiltration, Water Res. 44 (12) (2010) 3607–3616, https://doi.org/10.1016/j.watres.2010.04.020.
[38] Simon Judd, The MBR Book: Principles and Applications of Membrane Bioreactors for Water and Wastewater Treatment, Elsevier, 2010.
[39] DOW, Water & Process Solutions, FILMTEC™ Reverse Osmosis Membranes: Technical Manual, Dow Chem. Co, 2013, p. 181, in: http://www.dow.com/en-us/water-and-process-solutions/products/reverse-osmosis#/accordion/F36C1D89-9385-480A-9242-575D600E6F81 (Accessed date: 2 July 2018).
[40] X. Wu, Y. Li, Z. Su, L. Tian, M.S. Siddique, W. Yu, Less pressure contributes to gravity-driven membrane ultrafiltration with greater performance: enhanced driving efficiency and reduced disinfection by-products formation potential, J. Environ. Sci. 137 (2023) 407–419, https://doi.org/10.1016/j.jes.2023.02.049.
[42] P. Teta Prihartini Aryanti, F. Adi Nugroho, N. Anwar, R. Lestary, I. Badriyah, E. Ardi Ronaldi, PVC-based gravity driven ultrafiltration membrane for river water treatment, Mater. Today Proc. 87 (2023) 253–258, https://doi.org/10.1016/j.matpr.2023.03.103.
[44] N. Figueras, J. Matas, R. García-Pacheco, Tratamiento de agua residual con filtros reciclados, Universitat de Girona, 2022.
[45] D. Stoffel, N. Derlon, J. Traber, C. Staaks, M. Heijnen, E. Morgenroth, Gravity-driven membrane filtration with compact second-life modules daily backwashed: an alternative to conventional ultrafiltration for centralized facilities, Water Res. X 18 (2023) 100178, https://doi.org/10.1016/j.wroa.2023.100178.
[46] V.R. Moreira, Y.A.R. Lebron, L.V. de Souza Santos, M.C.S. Amaral, Low-cost recycled end-of-life reverse osmosis membranes for water treatment at the point-of-use, J. Clean. Prod. 362 (2022) 132495, https://doi.org/10.1016/j.jclepro.2022.132495.
[47] S. Molina, J. Landaburu-Aguirre, L. Rodríguez-Sáez, R. García-Pacheco, J.G. de la Campa, E. García-Calvo, Effect of sodium hypochlorite exposure on polysulfone recycled UF membranes and their surface characterization, Polym. Degrad. Stab. 150 (2018) 46–56, https://doi.org/10.1016/j.polymdegradstab. 2018.02.012.
[49] R. García-Pacheco, J. Landaburu-Aguirre, A. Lejarazu-Larrañaga, L. Rodríguez-Sáez, S. Molina, T. Ransome, Free chlorine exposure dose (ppm·h) and its impact on RO membranes ageing and recycling potential, Desalination 457 (2019) 133–143, https://doi.org/10.1016/j.desal.2019.01.030.
[50] R. García-Pacheco, J. Landaburu-Aguirre, S. Molina, L. Rodríguez-Sáez, S.B. Teli, E. García-Calvo, Transformation of end-of-life RO membranes into NF and UF membranes: evaluation of membrane performance, J. Membr. Sci. 495 (2015) 305–315, https://doi.org/10.1016/j.memsci.2015.08.025.
[51] J. Wu, B. Jung, A. Anvari, S. Im, M. Anderson, X. Zheng, Reverse osmosis membrane compaction and embossing at ultra-high pressure operation, Desalination 537 (2022) 115875, https://doi.org/10.1016/j.desal.2022.115875.
[52] A. Schäfer, N. Andritsos, A.J. Karabelas, E.M.V. Hoek, R. Schneider, M. Nyström, Fouling in Nanofiltration, Elsevier, 2004. https://era.ed.ac.uk/handle/1842/4271.
[53] BOE-A-2007-21092 Real Decreto 1620/2007, de 7 de diciembre, por el que se establece el régimen jurídico de la reutilización de las aguas depuradas, Retrieved February 21, 2024, from, https://www.boe.es/buscar/act.php?id=BOE-A-2007-21092.
[54] O. Radley-Gardner, H. Beale, R. Zimmermann (Eds.), Fundamental Texts on European Private Law, Hart Publishing, 2016, https://doi.org/10.5040/9781782258674.